24 July 2002

Chemical Physics Letters 361 (2002) 49–56

CHEMICAL PHYSICS LETTERS

www.elsevier.com/locate/cplett

# UV resonance Raman studies of ClNO in solution

Bethany P. Barham, Philip J. Reid *

*Department of Chemistry, P.O. Box 351700, University of Washington, Seattle, WA 98195, USA*

Received 2 April 2002; in final form 15 May 2002

**Abstract**

The first resonance Raman spectra of nitrosyl chloride (ClNO) in solution obtained with excitation resonant with the A-band are reported. For ClNO dissolved in cyclohexane, intensity is observed for transitions corresponding to all three normal coordinates: the bend, NCl stretch and NO stretch. This observation demonstrates that excited-state structural evolution occurs along these coordinates following photoexcitation resonant with the A-band. Resonance Raman depolarization ratios measured at excitation wavelengths spanning the A-band are reported. The depolarization ratios are found to be less that 1/3 consistent with at least two electronic transitions contributing to the A-band absorption intensity. 

## 1. Introduction

The photochemistry of nitrosyl halides such as nitrosyl chloride (ClNO) is of interest due to the participation of these compounds in stratospheric and tropospheric chemistry [1,2]. ClNO is formed in the lower atmosphere by the reaction of sea salt (NaCl) with $NO_2$, and in the upper troposphere/stratosphere via surface reactions of HONO on frozen HCl. In the gas-phase, the photochemistry of ClNO is dominated by dissociation to NO and Cl which occurs with near-unity quantum yield [1,3–14]:

$$\mathrm{ClNO} \xrightarrow{h\nu} \mathrm{NO}(^2\Pi_{\pm 1/2,\pm 3/2}) + \mathrm{Cl}(^2\mathrm{P}_{1/2,3/2})$$

The visible-ultraviolet (UV) absorption spectrum of ClNO is characterized by a series of absorption bands extending from ~650 nm into the UV [15,16]. Consistent with earlier studies, these bands are referred to as the K–A bands as one proceeds from low to high energy. Studies of gaseous ClNO have provided a detailed understanding of the dissociation dynamics that occur following photoexcitation resonant with all transitions except for the A-band ($\lambda_{max} = 196$ nm) [17,18]. The substantial cross-section and breadth of the A-band suggests that more than a single electronic transition contributes to the observed band intensity. Consistent with this suggestion, photodissociation studies have observed an evolution in photofragment anisotropy with increased actinic energy consistent with multiple states participating in the dissociation dynamics [11,13]. It should be noted that an evolution in photoproduct anisotropy can occur when a substantial amount of energy is deposited into rotational energy of diatomic fragment, even when a single-state is involved in the photochemistry [19–21]. However, studies of the

* Corresponding author. Fax: +206-685-8665.
*E-mail address:* preid@chem.washington.edu (P.J. Reid).

0009-2614/02/$ - see front matter 
PII: S0009-2614(02)00920-X

Cl-product velocity distribution have demonstrated that the anisotropy is independent of the kinetic energy released into the products consistent with the multiple-state model [14]. From a theoretical perspective, ab initio studies have predicted the presence of multiple transitions in this wavelength region [7,22,23]. However, recent UV resonance Raman studies of gaseous OClO found that the evolution in scattering intensity with excitation wavelength could be interpreted in terms of a single-state dominating the A-band intensity [24]. Therefore, the number of electronic states participating in the photodissociation dynamics of gaseous ClNO following A-band excitation remains unclear.

In contrast to the gas-phase, information regarding ClNO photochemistry in condensed environments is limited. Studies of ClNO surface photochemistry have observed NO formation suggesting that similar to the gas-phase, photoexcitation leads predominately to N–Cl bond cleavage [25]. However, matrix isolation studies have observed the formation of ClON following ClNO photoexcitation suggesting that photoisomerization may also occur in condensed environments [26,27]. Matrix isolation studies of ClNO:water complexes have also demonstrated the formation of HONO/HCl [28]. Finally, the photochemical reaction dynamics of ClNO in solution are essentially unknown.

We have been using resonance Raman intensity analysis to study the solution-phase excited-state reaction dynamics of ClNO that occur following A-band photoexcitation. Earlier Raman spectra of gaseous and matrix isolated ClNO were obtained using excitation wavelengths that were non-resonant or pre-resonant with the A-band [29–31]. In these studies, differences in transition frequencies were observed for gas-phase versus matrix-isolated ClNO suggesting that the ground-state potential energy surface is sensitive to environment. Recently, resonance Raman spectra of gaseous ClNO employing A-band excitation were reported [24]. Scattering corresponding to the bend and NCl-stretch coordinates was observed demonstrating that excited-state structural evolution occurs along these coordinates following photoexcitation. Scattering corresponding the NO-stretch was not observed suggesting that structural evolution does not occur along this coordinate following A-band excitation. A corresponding study of ClNO in solution would show how the presence of solvent impacts these dynamics.

We report here the first resonance Raman spectra of ClNO in solution. Specifically, resonance Raman spectra of ClNO dissolved in cyclohexane employing excitation resonant with the A-band are presented. Cyclohexane was chosen for study since the absorption spectrum of ClNO is minimally shifted in this solvent relative to the gas-phase. Therefore, this solvent provides an environment somewhat comparable to that of gaseous ClNO. The results presented here show that significant intensity is observed for transitions involving the NCl stretch consistent with dissociative evolution along this coordinate upon photoexcitation. We also provide the first evidence for resonance Raman intensity corresponding to the NO stretch consistent with modest excited-state structural evolution along this coordinate. As mentioned above, it has been proposed that the A-band is comprised of more than one electronic transition. The presence of multiple transitions can be investigated using resonance Raman depolarization ratios. A depolarization ratio of a 1/3 suggests that a single-state makes the dominant contribution to the observed scattering, and deviations from this value provide evidence that multiple states contribute to the observed scattering. We have found that the ClNO depolarization ratios are less than 1/3 consistent with the A-band being composed of more than a single electronic transition.

## 2. Experimental

### 2.1. Materials

Nitrosyl chloride (ClNO) was synthesized using literature methods [32]. Briefly, 8.75 g of sodium nitrite (99.9% reagent grade, Aldrich) was dissolved in 12.5 ml of water, and added drop-wise to 50 ml of concentrated hydrochloric acid (Fisher). The solution was stirred continuously, and the production of ClNO was evidenced by the evolution of

an orange-brown gas. The ClNO gas passed through a condenser and drying tube packed with sodium nitrite (99.9% reagent grade, Aldrich), moist potassium chloride (Baker), and calcium chloride (Fisher). The product gas was collected in a flask submerged in a dry ice/acetone bath, resulting in a deep red/bright yellow liquid slurry of ClNO (boiling point: −6 °C). ClNO was allowed to warm, and the gaseous ClNO produced upon warming was bubbled through cyclohexane to produce the ClNO/cyclohexane stock solution. Purity was determined by static vis-UV absorption. To construct the sample, the stock solution was diluted until a ClNO concentration of 0.1–4 mM was reached, the specific concentration depending on excitation wavelength. Stock solutions were made approximately once a week to ensure sample integrity.

The absorption cross-section for ClNO in cyclohexane was determined as follows. The preparation of ClNO was performed as described above, and neat ClNO was isolated as a liquid using a dry ice/acetone bath. Calibrated capillary pipettes were precooled in liquid nitrogen and used to transfer the liquid ClNO into volumetric flasks for dilution and determination of the cross-section.

### 2.2. Resonance Raman spectra

Excitation wavelengths of 282.4, 252.7, 228.7, 217.8 and 192.2 nm were obtained from the hydrogen shifted, second and third harmonic output from a Nd:YAG laser (Spectra Physics GCR 170). ClNO in cyclohexane was flowed through a quartz cell equipped with sapphire windows. The sample flow rate was sufficient to replace the illuminated sample volume between excitation pulses. The scattered light was collected by refractive UV-quality optics and delivered to a 0.75-m spectrograph (Acton) where it was dispersed using either a 1200-groove/mm classically ruled, 2400-groove/mm holographic, or 3600-g/mm holographic grating. Detection of the scattered light was accomplished using a $1100 \times 300$ pixel, back-thinned, liquid nitrogen cooled CCD detector (Princeton Instruments). A HP diode array spectrometer was used to monitor the sample concentrations (0.1–4 mM for ClNO) before and after each experiment. The concentration changed less than 10% for a single experiment. All ClNO scattering intensities were found to increase linearly with incident power.

### 2.3. Depolarization ratios

Resonance Raman depolarization ratios were determined at 282.4, 252.7, 228.7 and 217.8 nm. The depolarization ratio is defined as the intensity of scattered light with polarization perpendicular to that of the excitation light divided by the intensity of scattered light with polarization parallel to that of the excitation light [33]. An α-BBO-polarizer was put in the path of the excitation beam to define the incident polarization. Also, the sapphire windows on the sample cell were replaced with non-birefringent $CaF_2$ windows to maintain the polarization of the incident and scattered fields. The polarization of the scattered light was analyzed using a large aperture (1.5 cm) Glan–Taylor calcite polarizer placed before the polarization scrambler at the entrance to the spectrograph. Measurement of the depolarization ratio of the 802 $cm^{-1}$ cyclohexane transition was performed at each wavelength to correct for the non-ideal extinction of the polarizer as described in detail elsewhere [34]. Transition intensities were determined by both simple peak integration and by fitting the bands to a Gaussian function convolved with a Lorenztian instrument response. Either approach was found to produce identical results within the experimental error.

## 3. Results and discussion

### 3.1. Absorption spectra

Fig. 1 presents the absorption spectrum of gaseous ClNO, and of ClNO dissolved in cyclohexane. The large transition observed in this wavelength region is commonly referred to as the A-band [15,16]. The breadth and absence of structure for this transition suggests that rapid dissociation occurs following photoexcitation resonant with this transition. The gas-phase spectrum is in agreement with that reported in the literature

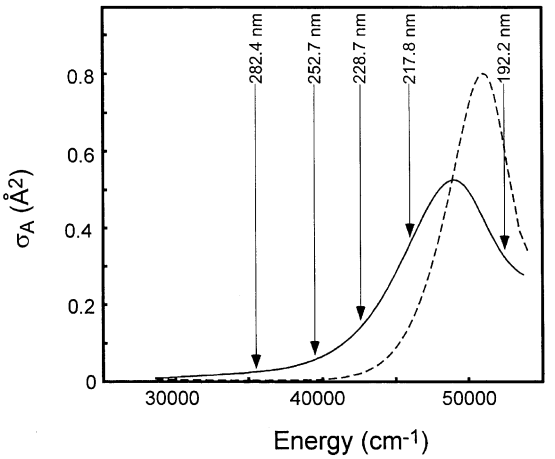


Fig. 1. Absorption spectrum of ClNO in cyclohexane (solid) and in gas-phase (dotted). Excitation wavelengths employed in this study are indicated.

[16]. The maximum absorption cross-section of ClNO in cyclohexane was determined to be 0.48 $\text{Å}^2$ at 48 500 $\text{cm}^{-1}$ ($\lambda_{max} = 206$ nm). Comparison of the gas-phase and cyclohexane spectra demonstrates that the absorption maximum is shifted 2480 $\text{cm}^{-1}$ (10 nm) to lower energy in cyclohexane. In addition, the transition becomes broader in cyclohexane (~9000 $\text{cm}^{-1}$ full-width at half maximum); however, the integrated intensity of the A-band in both the gas and condensed phase is the same (within experimental error). This suggests that the increased breadth is not due to the appearance of a new electronic transition, but is instead due to a change in the energetics and/or displacements of excited-state or states involved in the electronic transitions that comprise the A-band.

### 3.2. ClNO in cyclohexane Raman intensity analysis

Representative resonance Raman spectra of ClNO dissolved in cyclohexane obtained with excitation at 282.4, 217.8 and 192.2 nm are presented in Fig. 2. The location of these excitation wavelengths with respect to the A-band is indicated in Fig. 1. Inspection of Fig. 2 demonstrates that the spectra are dominated by intensity corresponding to the bend and NCl stretch, similar to the behavior observed for gaseous ClNO [24]. Mode

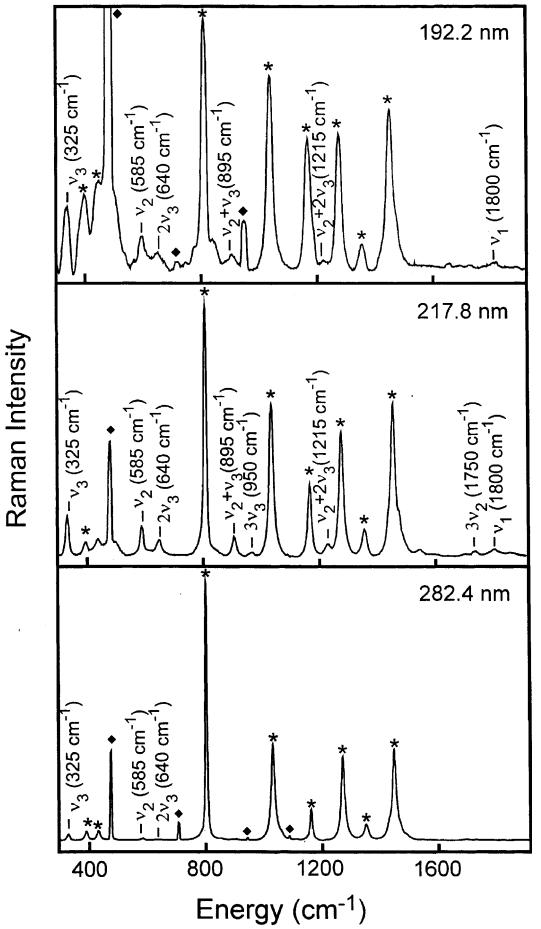


Fig. 2. Resonance Raman spectrum of ClNO in cyclohexane obtained at 282.4, 217.8 and 192.2 nm excitation. Solvent lines are marked with asterisks and hydrogen lines are denoted with diamonds. Note that directly on resonance (217.8 and 192.2 nm) transitions corresponding to all three vibrational modes ($\nu_1$, NO stretch, $\nu_2$, NCl stretch and $\nu_3$, bend) are observed.

assignments and descriptions employed here are in agreement with those described by Bell et al. and others; [26,30,31] however, other mode assignments have been proposed [24]. The transition frequencies observed in cyclohexane, and those reported for gaseous ClNO are presented in Table 1. Comparison of the transition frequencies demonstrates that the frequencies in cyclohexane are reduced by approximately 10–20 $\text{cm}^{-1}$ relative to the gas-phase demonstrating that the ground-state potential energy surface is significantly modified in solution. In addition to transitions involving the

Table 1
Resonance Raman transition frequencies for ClNO dissolved in cyclohexane and gaseous ClNO

| Transition | Transition frequency in cyclohexane ($cm^{-1}$) | Transition frequency in the gas-phase[a] ($cm^{-1}$) |
|---|---|---|
| $\nu_3$ | 325 | 330 |
| $\nu_2$ | 585 | 598 |
| $2\nu_3$ | 640 | 662 |
| $\nu_2 + \nu_3$ | 895 | 926 |
| $3\nu_3$ | 950 | 984 |
| $2\nu_2$ | | 1184 |
| $\nu_2 + 2\nu_3$ | 1215 | 1249 |
| $2\nu_2 + \nu_3$ | | 1506 |
| $\nu_2 + 3\nu_3$ | | 1569 |
| $5\nu_3$ | | 1640 |
| $3\nu_2$ | 1750 | 1768 |
| $\nu_1$ | 1800 | |

[a] Taken from [24].

bend and NCl stretch, resonance Raman intensity corresponding to the NO stretch is also observed (1800 $cm^{-1}$). These data represent the first observation of resonance Raman intensity involving this coordinate. The pattern of resonance Raman intensities observed here demonstrates that excited-state structural evolution occurs along all three vibrational coordinates upon photoexcitation. Although the NO-stretch fundamental transition is observed, attempts to observe the corresponding overtone transitions were unsuccessful suggesting that only modest evolution occurs along this coordinate upon A-band photoexcitation. Therefore, the resonance Raman results presented here demonstrate that the initial excited-state structural evolution of ClNO is dominated by evolution along the bend and NCl stretch with only modest evolution occurring along the NO stretch.

It has been proposed that the A-band is comprised of more than a single electronic transition. In photodissociation studies employing 193 nm excitation, Haas et al. [11] observed a bimodal NO-fragment energy distribution with differing photoproduct recoil anisotropies suggesting that two electronic transitions are in close proximity at this excitation wavelength. This hypothesis was further explored in subsequent studies by Felder and Morley [13] where the observation of distinct photofragment anisotropy and energy distributions following photoexcitation at 248 nm led them to conclude that the A-band is comprised of more than one excited-state. Photofragmentation studies of Skorokhodov et al. [14] employing excitation at 235 nm observed the production of ground and spin–orbit excited Cl with a bimodal distribution of translational energy. This result taken in combination with earlier studies resulted in a three-state model for the A-band. Finally, ab initio studies predict that multiple states lie in the energetic vicinity of A-band; however, two singlet–singlet transitions are expected to carry the majority of the oscillator strength [7,23].

Understanding the dissociation dynamics that occur following A-band photoexcitation is dependent on identifying the number of states that participate in the dissociation process. This issue can be addressed through the measurement and analysis of resonance Raman depolarization ratios. The resonance Raman depolarization ratio is defined as the intensity of scattered light with polarization perpendicular to that of the excitation light divided by the intensity of light scattered with polarization parallel to that of the excitation light. The simplest two-state model for the A-band consistent with the ab initio results is obtained in the limit where the A-band is comprised of two orthogonal transitions with no vibronic coupling between these surfaces. In this limit, the depolarization ratio ($\rho$) expressed as polarizability tensor elements is defined as [33]:

$$\rho = \frac{I_{\mathrm{per}}}{I_{\mathrm{par}}} = \frac{3\Sigma^2}{10\Sigma^0 + 4\Sigma^2},$$

where

$$\Sigma^0 = \frac{1}{3}\left|\alpha_{xx} + \alpha_{yy}\right|^2,$$

$$\Sigma^2 = \frac{1}{3}\left\{\left|\alpha_{xx} - \alpha_{yy}\right|^2 + \left|\alpha_{xx}\right|^2 + \left|\alpha_{yy}\right|^2\right\}.$$

These expressions are representative of the following picture. The presence of two-electronic transitions gives rise to two corresponding elements of the polarizability tensor ($\alpha_{xx}$ and $\alpha_{yy}$). If the A-band were comprised of a single electronic transition, then only a single tensor element would be non-vanishing and $\rho = 1/3$. To the extent a second, orthogonal transition contributed to

Table 2
Depolarization ratios for ClNO in cyclohexane

| Excitation wavelength (nm) | $\rho(\nu_3)$[a] | $\rho(\nu_2)$ | $\rho(2\nu_3)$ |
|---|---|---|---|
| 282.4 | $0.19 \pm 0.02$[b] | $0.21 \pm 0.03$ | $0.33 \pm 0.06$ |
| 252.7 | $0.20 \pm 0.03$ | $0.13 \pm 0.01$ | $0.16 \pm 0.04$ |
| 228.7 | $0.20 \pm 0.02$ | $0.09 \pm 0.01$ | $0.13 \pm 0.04$ |
| 217.8 | $0.22 \pm 0.01$ | $0.11 \pm 0.01$ | $0.13 \pm 0.01$ |

[a] Raman depolarization ratios are defined as the scattered intensity with polarization perpendicular to that of the incident radiation divided by the scattered intensity with polarization parallel to that of the incident radiation.

[b] Errors represent one standard deviation from the mean 3–5 measurements depending on excitation wavelength.

A-band intensity, the second tensor element becomes appreciable and $\rho \neq 1/3$. The depolarization ratios for the NCl stretch ($\nu_2$), the bend ($\nu_3$), and the bend overtone ($2\nu_3$) transitions measured at 282.4, 252.7, 228.7 and 217.8 nm are presented in Table 2 and depicted in Fig. 3. The figures demonstrate that the depolarization ratios are significantly less than 1/3 consistent with more than one excited-state contributing to the observed scattering.

It should be noted that the deviation of the depolarization ratios from the single-state limit of 1/3 could reflect pre-resonance contributions from states located in the far-UV. The importance of this effect was studied by calculating the expected depolarization dispersion curve for the bend fundamental transition by modeling the A-band as being due to a single electronic transition, and employing a pre-resonant expression to model polarizability contributions from states located in the far-UV. The polarizability contribution of the single-state involved in the A-band transition was determined using the time-dependent formalism as described in detail elsewhere [34]. Parameters for this state were chosen such that the breadth of the absorption spectrum and absolute scattering cross-sections for the bend fundamental transition were reproduced. The pre-resonant contribution from the far-UV state was modeled using the following expression:

$$\alpha(E_1) = M_{eg}^2 \frac{\omega}{\sqrt{2}} \Delta \frac{E_{00}^2 + E_1^2}{(E_{00}^2 - E_l^2)^2},$$

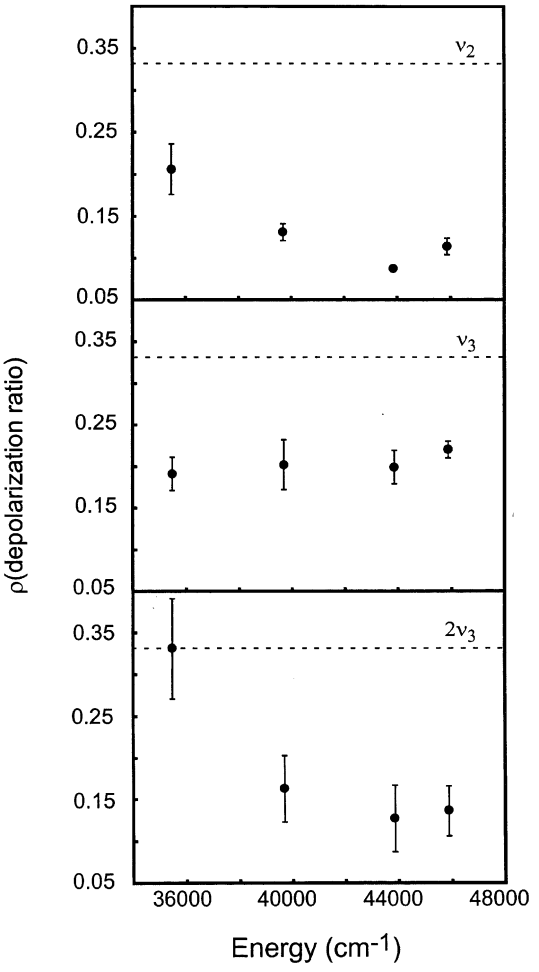


Fig. 3. Depolarization ratios versus excitation wavelength for NCl-stretch fundamental ($\nu_2$), the bend ($\nu_3$), and the bend overtone ($2\nu_3$).

where $M_{eg}$ is transition length for the transition of interest, $\omega$ is mode frequency, $\Delta$ is the displacement of the excited-state potential energy surface minimum relative to the ground state along the coordinate of interest, $E_{00}$ is the energy of the excited-state from which the pre-resonant intensity is derived, and $E_1$ is the incident field energy. The far-UV absorption spectrum of ClNO demonstrates transition intensity at ~150 nm with a cross-section that is roughly half that of the A-band [35]. Therefore values of $E_{00} = 65\,000$ cm$^{-1}$ and $M_{eg} = 0.2$ Å were employed. Using the ground-state frequency of the bend (325 cm$^{-1}$),

values of $\Delta$ ranging from 0.25 to 2.5 were investigated. A representative fit to the depolarization dispersion data for the bend fundamental transition employing this model for $\Delta = 1.0$ is presented in Fig. 4a. The agreement between theory and experiment is poor, and demonstrates that pre-resonance contributions from states located in the far-UV are incapable of reproducing the observed depolarization ratios. Furthermore, pre-resonant contributions are expected to cause little or no deviation to the depolarization dispersion curve in this wavelength region of the A-band.

We have also performed a preliminary calculation in which the A-band is modeled as being comprised of two orthogonal transitions. Fig. 4b presents the results for this two-state model with

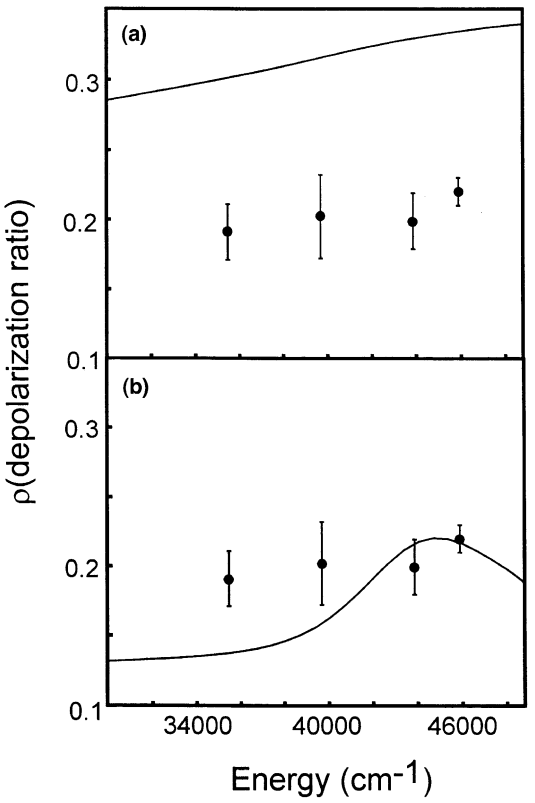


Fig. 4. Depolarization dispersion curves for the bend fundamental transition derived using the resonant/pre-resonant (a) and a two-resonant-state models (b) for the A-band. Experimental bend depolarization ratios (points) are indicated. Details of the models are presented in the text.

$E_{00} = 34\,500$ cm$^{-1}$ and $M_{eg} = 0.8$ for state 1, and $E_{00} = 39\,200$ cm$^{-1}$ and $M_{eg} = 0.82$ for state 2. In addition, displacements along the all three coordinates were taken to be equal in both states, and adjusted to reproduce the breadth of the overall absorption band as well as the absolute scattering cross-sections for the bend and N–Cl stretch. The agreement between the model and experiment is good, and demonstrates that a two-state model is capable of reproducing the depolarization date for excitation wavelengths directly resonant with the A-band. Ratios measured at lower excitation energies are underestimated in the model potentially due to contributions from the weak B-band at these wavelengths. The comparison between the data and two-state model clearly demonstrates that the resonance Raman depolarization ratios are consistent with the A-band being comprised of at least two electronic transitions. We are currently developing a two-state model for the A-band that is capable of reproducing the absorption spectrum, absolute scattering cross-sections, and depolarization ratios.

## 4. Conclusion

We have presented the first resonance Raman spectra of ClNO in solution. The spectra of ClNO dissolved in cyclohexane demonstrate that significant structural evolution occurs along the bend and NCl stretch upon A-band photoexcitation. For the first time, resonance Raman intensity corresponding to the NO-stretch coordinate was observed; however, the limited intensity for this transition suggests that the excited-state structural evolution that occurs along this coordinate following photoexcitation is modest. Finally, resonance Raman depolarization ratios were obtained and found to be consistent with the A-band being comprised of at least two separate electronic transitions. Currently, resonance Raman intensity analysis studies are underway to observe ClNO in additional solvents, and to determine depolarization ratios at other excitation wavelengths in an attempt to obtain a mode-specific model of the excited-states that comprise the A-band.

## Acknowledgements

The National Science Foundation is acknowledged for their support of this work (CHE-0091320). Acknowledgment is also made to the donors of the Petroleum Research Fund, administered by the American Chemical Society. P.J.R. is the recipient of an Alfred P. Sloan Fellowship, and is a Cottrell Scholar of the Research Corporation.

## References

[1] C.B. Colburn, Developments in Inorganic Nitrogen Chemistry, Elsevier Scientific Publishing Company, New York, 1973.
[2] B.J. Finlayon-Pitts, J.N. Pitts, Chemistry in the Upper and Lower Atmosphere, Academic Press, New York, 2000.
[3] R. Engelman, P.E. Rouse, J. Mol. Spectrosc. 37 (1971) 240.
[4] M.D. Moser, E. Weitz, G.C. Schatz, J. Chem. Phys. 78 (1983) 757.
[5] J. Bechara, T. Morrow, W.D. McGrath, Chem. Phys. Lett. 122 (1985) 605.
[6] A. Ticktin, A.E. Bruno, U. Bruhlmann, J.R. Huber, Chem. Phys. 125 (1988) 403.
[7] Y.Y. Bai, A. Ogai, L. Iwata, G.A. Segal, H. Reisler, J. Chem. Phys. 90 (1989) 3903.
[8] A. Ogai, C.X.W. Qian, H. Reisler, J. Chem. Phys. 93 (1990) 1107.
[9] C.X.W. Qian, A. Ogai, L. Iwata, H. Reisler, J. Chem. Phys. 92 (1990) 4296.
[10] J. Cao, Y. Wang, C.X.W. Qian, J. Chem. Phys. 103 (1995) 9653.
[11] B.M. Haas, P. Felder, J.R. Huber, Chem. Phys. Lett. 180 (1991) 293.
[12] I.T.F. Gillan, D.J. Denvir, H.F.J. Cormican, I. Duncan, T. Morrow, Chem. Phys. 167 (1992) 193.
[13] P. Felder, G.P. Morley, Chem. Phys. 185 (1994) 145.
[14] V. Skorokhodov, Y. Sato, K. Suto, Y. Matsumi, M. Kawasaki, J. Phys. Chem. 100 (1996) 12321.
[15] C.F. Goodeve, S. Katz, Proc. R. Soc. A 172 (1939) 432.
[16] N.M. Ballash, D.A. Armstrong, Spectrochim. Acta 30A (1974) 941.
[17] H. Reisler, C. Qian, in: J.M. Bowman (Ed.), Advances in Molecular Vibrations and Collision Dynamics, vol. 1B, JAI Press, Greenwich, 1991, p. 231.
[18] C.X.W. Qian, A. Ogai, J. Brandon, Y.Y. Bai, H. Reisler, J. Phys. Chem. 95 (1991) 6763.
[19] H.P. Loock, J. Cao, C.X.W. Qian, Chem. Phys. Lett. 206 (1993) 422.
[20] A.V. Demyanenko, V. Dribinski, H. Reisler, H. Meyer, C.X.W. Qian, J. Chem. Phys. 111 (1999) 7383.
[21] S.H. Kable, J.-C. Loison, D.W. Neyer, P.L. Houston, I. Burak, R.N. Dixon, J. Phys. Chem. 95 (1991) 8013.
[22] D. Solgadi, F. Lahmani, C. Lardeux, Chem. Phys. 79 (1983) 225.
[23] S. Lacombe, M. Loudet, A. Dargelos, J.M. Camou, Chem. Phys. 258 (2000) 1.
[24] J.L. Mackey, B.R. Johnson, C. Kittrell, L.D. Lee, J.L. Kinsey, Chem. Phys. 114 (2001) 15.
[25] C. Ning, J. Pfab, Chem. Phys. Lett. 216 (1993) 87.
[26] A. Hallou, L. Schriver-Mazzuoli, A. Schriver, P. Chaquin, Chem. Phys. 237 (1998) 251.
[27] G. Maier, H.P. Reisenauer, M. De Marco, Chem. Eur. 6 (2000) 800.
[28] A. Pieretti, N. Sanna, A. Hallou, L. Schriver-Mazzuoli, A. Schriver, J. Mol. Struct. 447 (1998) 223.
[29] J.K. McDonald, J.A. Merritt, V.F. Kalasinsky, H.L. Huesel, J.R. Durig, J. Mol. Spectrosc. 117 (1986) 69.
[30] A.J. Bell, P.R. Pardon, J.G. Frey, Mol. Phys. 67 (1989) 465.
[31] A.J. Bell, J.G. Frey, Mol. Phys. 69 (1990) 943.
[32] G. Pass, H. Sutcliffe, Practical Inorganic Chemistry: Preparation, Reactions and Instrumental Methods, Chapman and Hall, London, 1968.
[33] O.S. Mortensen, S. Hassing, in: R.E. Hester, R.J.H. Clark (Eds.), Advances in Infrared and Raman Spectroscopy, vol. 6, Heyden, London, 1980, p. 1.
[34] P.J. Reid, A.P. Esposito, C.E. Foster, R.A. Beckman, J. Chem. Phys. 107 (1997) 8262.
[35] H. Okabe, in: Photochemistry of Small Molecules, Wiley-Interscience, New York, 1978, p. 170.